

◆ 특집 ◆ 최신 정밀 설계재료 기술 II

몽크만 · 그랜트관계에 기초한 소형펀치 크리프시험 데이터와 일축 크리프시험 데이터의 관계

Relationship Between Small-punch Creep Test Data and Uniaxial Creep Test Data based on the Monkman–Grant Relation

김범준^{1,✉}, 손일선², 임병수³

Bum Joon Kim^{1,✉}, Ilseon Sohn², and Byeong Soo Lim³

¹ 오산대학교 기계공학과 (Department of Mechanical Engineering, Osan Univ.)

² 오산대학교 자동차공학과 (Department of Automotive Engineering, Osan Univ.)

³ 성균관대학교 기계공학과 (School of Mechanical Engineering, Sungkyunkwan Univ.)

✉ Corresponding author: kultra@osan.ac.kr, Tel: +82-31-370-2662, Fax: +82-31-370-2669

Manuscript received: 2013.5.31 / Revised: 2013.7.13 / Accepted: 2013.7.16

The relationship between the small-punch creep test and the conventional creep test was investigated experimentally using a method similar to that of the Monkman–Grant relationship. Uniaxial and small-punch creep rupture tests were carried out on 9Cr-2W ferritic steel (Commercial Grade 92 steel: X10CrWMoVNb 9-2) at elevated temperatures. From the relation derived in the same manner as the Monkman–Grant relation, a correlation between the displacement rate in response to the small-punch creep test and the strain rate in the uniaxial creep test was found, and the creep life was calculated using this relation. Furthermore, the failure modes of the small punch creep test specimens were investigated to show that the fracture was caused by creep.

Key Words: Uniaxial creep (일축 크리프), Small-punch creep (소형펀치 크리프), Monkman–Grant relation (몽크만-그랜트관계), Minimum creep rate (최소크리프 속도)

NOMENCLATURE

ϵ : Strain

δ : Displacement

t_R : Time to rupture

1. Introduction

It is very difficult and potentially dangerous to extract a uniaxial creep specimen from an in-service component,

owing to the specimen size required by the ASTM or ASME standards. The small punch creep (SPC) test has been developed as a useful method suitable for measuring creep characteristics using miniaturized disc specimens extracted from service components during their operation.¹⁻³ Therefore, it could be considered a substitute for the uniaxial creep-rupture test by which the residual creep life can be measured; moreover, its utility and merits have been established.⁴⁻⁸ Generally, a uniaxial creep specimen is tested under uniaxial stress, whereas

the SPC specimen is tested under multiaxial stress. In addition, the strain data in the SPC test have the dimensions of displacement (mm), while those in a uniaxial creep test are dimensionless (mm/mm).

The focus of this work was to investigate the relationship between the SPC test data and uniaxial creep test data by an analysis similar to that of the Monkman–Grant relationship, using experimentally acquired test data. Thus, the creep behavior of 9Cr-2W ferritic steel (Grade 92 steel: X10CrWMoVNb 9-2), which is used in USC (ultra super critical) fossil-fuel power plants, was studied at elevated temperatures. Creep tests were performed using the SPC tester at constant loads and a uniaxial creep tester at constant stress. The time to fracture and the minimum displacement rate measured during the SPC tests were related in a similar manner to the corresponding uniaxial creep test data. From the relation derived in the same manner as the Monkman–Grant relation, a correlation between the displacement rate in the SPC test and the strain rate in the uniaxial creep test was established and creep lives were evaluated using this relation. The fracture mechanism of SPC specimen was investigated by SEM.

2. Experimental Procedure

2.1 Small-punch creep test

In this study, Grade 92 steel, used as a heat-resistant steel in fossil-fuel power plants, was employed. Table 1 and 2 show the chemical composition of Grade 92 steel and its tensile properties at the temperature of 600°C, respectively.

The creep properties of Grade 92 steel were evaluated with a small-punch (SP) tester. Fig. 1 shows the SPC jig used in this study. The SPC jig consists of a puncher, ball, upper die, and lower die. The specimen is placed on the lower die; the upper die is assembled on the lower die; and finally, the specimen is clamped between the upper and lower dies by four clamping screws. The test loads are applied onto the SPC specimen by the ball through the puncher. The dimensions of the SPC specimens were $10 \times 10 \times 0.5 \text{ mm}^3$; they were machined from the Grade 92 steel block. Before testing, the specimens were mechanically polished to $0.1\mu\text{m}$ and the thickness was controlled to within $\pm 10\mu\text{m}$ with a digital micrometer.

Table 1 Chemical composition of Grade 92 steel

C	Si	Mn	P	S	Al	Cr	Cu
0.10	0.22	0.48	0.017	0.006	0.01	9.11	-
Ni	Mo	V	Nb	N	W	B	Fe
0.18	0.47	0.18	0.056	0.041	1.71	0.0029	Rem.

Table 2 Tensile properties of Grade 92 steel at 600°C

Poisson's ratio	0.3
Young's modulus	125 [GPa]
Yield strength	367 [MPa]
Tensile strength	443 [MPa]

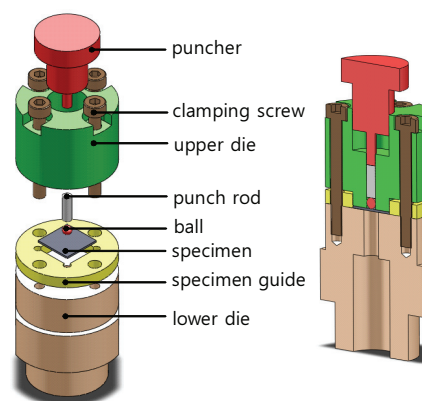


Fig. 1 Schematic illustration of SPC test apparatus

The SPC tests were performed in the temperature range of 600–700°C. The temperature of the SPC tester furnace was controlled to the accuracy of $\pm 1^\circ\text{C}$. Constant loads of 245.3–588.6N were applied onto the SPC specimens by the ceramic (Si_3N_4) ball, which had a diameter of 2.4 mm. All the tests were performed under atmospheric conditions to simulate the conditions of service components. The displacements of the specimens were measured by a linear variable displacement transducer (LVDT) to the accuracy of 10^{-3} mm . Table 2 shows the SPC test conditions.

2.2 Uniaxial creep test

To compare the results of the SPC tests, uniaxial creep-rupture tests were performed. The creep-rupture tests were carried out using a lever-arm-type creep tester equipped with an LVDT for the measurement of the displacement. Constant stresses of 169–265.6 MPa were applied at temperatures ranging from 600 to 650°C. As

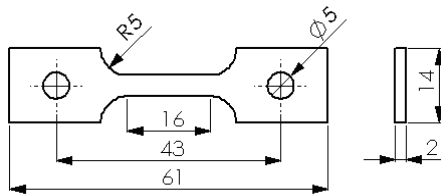


Fig. 2 Schematic diagram of uniaxial creep test specimen (unit: mm)

shown in Fig. 2, plate-shaped creep-rupture specimens were prepared and tested according to ASTM E 139. The specimens were heated using a three-zone-type furnace with the control accuracy of $\pm 1^\circ\text{C}$ in the test region.

2.3 Conversion method by modified Monkman-Grant relation

To convert the SPC displacements into uniaxial creep strains, the conversion methods on the modified Monkman-Grant relation and equations by Doveš, F. and Milička, K⁹ were used and their results analyzed for SPC.

The conversion method⁹ is as follows: The Monkman-Grant equation for a uniaxial creep test and the applied Monkman-Grant equation for a SPC test may be expressed as in Eqs. (1) and (2), respectively.

$$\log t_R + m_c \log \dot{\epsilon}_M = C_c \quad (1)$$

where m_c and C_c are constants and $\dot{\epsilon}_M$ is the minimum creep rate.

$$\log t_R + m_s \log \dot{\delta}_M = C_s \quad (2)$$

where constants m_s and C_s ; $\dot{\delta}_M$ is the minimum displacement rate.

From Eqs. (1) and (2), the relationship between the applied stress in the conventional creep test and the applied force in the SPC test can be compared based on comparison of tests of the same rupture life. If the constants in Eqs. (1) and (2) are known and the rupture time, t_R is same in the two creep tests, then Eq. (3) is obtained.

$$\log \dot{\epsilon}_M = \frac{m_s}{m_c} \log \dot{\delta}_M + \frac{C_c - C_s}{m_c} \quad (3)$$

$$\dot{\epsilon}_M = 10^{(C_c - C_s) / m_c} \dot{\delta}_M \quad (4)$$

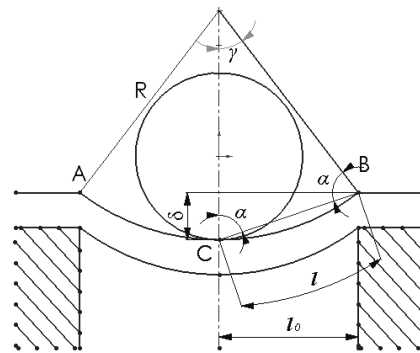


Fig. 3 Schematic diagram of SPC strain

Since the values of the parameters m_c and m_s are almost similar in both types of tests,¹⁰ Eq. (3) can be simplified to Eq. (4).

Then, the minimum displacement rate of SP creep can be converted into the minimum creep rate in the studied materials.

2.4 Conversion method by mechanical strength theory

From the viewpoint of mechanical strength theory, the displacement rate of SP creep was converted into the strain of conventional creep; the conversion method was as follows.

As shown in Fig. 3, the SPC specimens were deformed at their centers by the bending stress in the hole of the lower die. Here, it is supposed that the deformation in the cylindrical direction and thickness are negligible.

Therefore, from Fig. 3, the strain is described as Eq. (5).

$$\epsilon = (l - l_0) / l_0 \quad (5)$$

where m_c and C_c are constants and $\dot{\epsilon}_M$ is the minimum creep rate.

The deformed length, l can be derived by the circular measure from the relationship between \widehat{ABC} and $\angle\gamma$, as calculated in Eq. (6)

$$l = R\gamma \quad (6)$$

where R and γ are derived as in Eqs. (7) and (8), respectively.

Finally, Eq. (5) is derived as Eq. (9).

$$R = (\delta^2 + l_0^2) / 2\delta \tag{7}$$

$$\gamma = \sin^{-1}(l_0 / R) \text{rad} \tag{8}$$

$$\varepsilon = \left(\frac{(\delta_2 + l_0^2)}{2\delta} \cdot \gamma - l_0 \right) / l_0 \tag{9}$$

where δ is the deflection of the SP specimen shown in Fig. 3.

2.5 Fractography

To examine that the SPC fracture was caused by creep mechanism, the cross sectional area of SPC ruptured specimens was investigated.

3. Results and Discussion

3.1 Conversion results by mechanical strength theory

Figs. 4 and 5 show the results of the SPC and uniaxial creep tests at 600°C, respectively. Fig. 4 shows the typical displacement–time curves for Grade 92 steel obtained from the SPC tests; they are similar to the typical uniaxial creep curves shown in Fig. 5.

It shows the results of uniaxial creep tests at various stresses. From the viewpoint of mechanical strength theory, the SPC displacement in Fig. 4 was converted into the strain of conventional creep. As shown in Fig. 6, the converted creep strain curves are similar to the typical uniaxial creep curves.

Fig. 7 shows the comparison of the uniaxial Monkman–Grant and SPC Monkman–Grant relations which is calculated from the converted creep strain data of Fig. 6.

As shown in Fig. 7, the predicted creep-rupture life by the converted SP creep strain has not agreement with that by the uniaxial creep strain for the Monkman–Grant relation. This result is believed to be due to only mechanical bending mechanism without considering the effect of creep and plastic deformation.

3.2 Conversion results by modified Monkman–Grant relation

Fig. 8 shows the comparison of the uniaxial Monkman–Grant and SPC Monkman–Grant relations. As

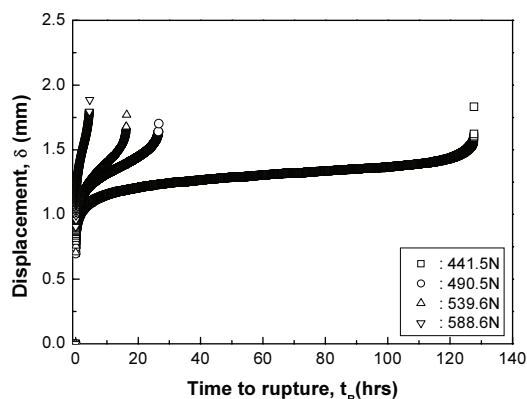


Fig. 4 Punch displacement vs. time curves

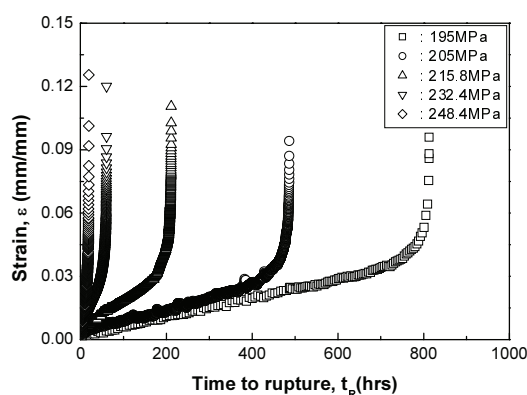


Fig. 5 Conventional strain vs. time curves

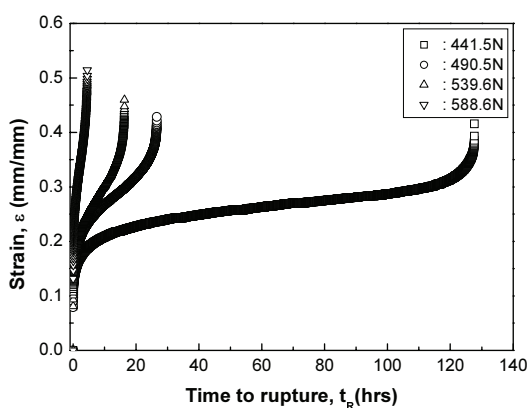


Fig. 6 Converted strain vs. time curves

shown in Fig. 8, the constants C_c and C_s were estimated to be equal to 0.028 and 0.539, and the exponent values, m_c and m_s , were found to be equal to 1.02 and 0.94 by linear regression, respectively. Generally, it is known that

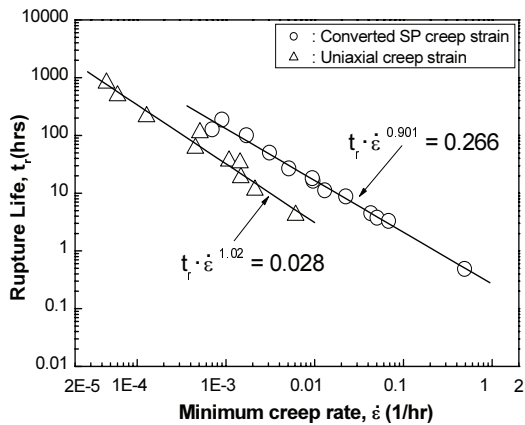


Fig. 7 Comparison of uniaxial Monkman–Grant and converted SPC Monkman–Grant relations

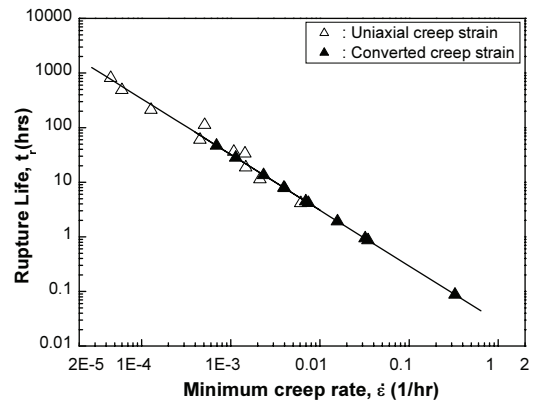


Fig. 9 Converted minimum creep rate by modified Monkman–Grant relations

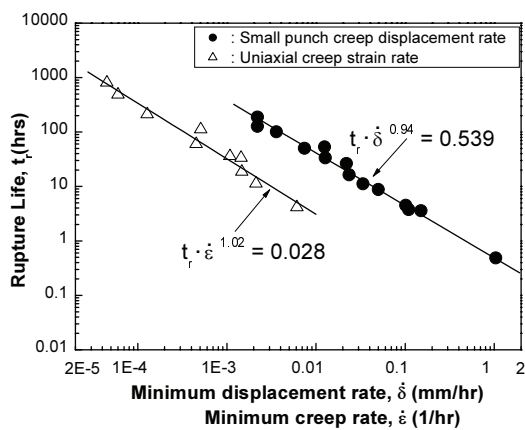


Fig. 8 Comparison of uniaxial Monkman–Grant relation and SPC modified Monkman–Grant relations

the exponent value of a Monkman–Grant equation, m , is equal to unity for most metallic alloys. For Grade 92 steel, the exponent values are near 1. From the modified Monkman–Grant equation, the provided values of the parameters m_c and m_s are almost similar in both tests. Finally, the equivalent relationship between the minimum creep rate and the minimum displacement rate is obtained as Eq. (10) for Grade 92 steels.

$$\dot{\epsilon}_M = 0.316 \dot{\delta}_M \quad (10)$$

Fig. 9 shows the predicted creep-rupture life on the basis of the Monkman–Grant relation derived by using Eq. (10).

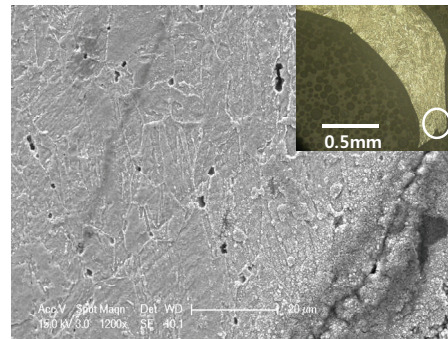


Fig. 10 Creep cavity formation at prior austenite grain boundaries(circle: observation area by SEM)

As shown in Fig. 9, the predicted creep-rupture life by the converted creep strain has good correlation with that by the uniaxial creep strain for the Monkman–Grant relation.

This result implies that the relation proposed by on the modified Monkman–Grant relation is valid for the studied steel, Grade 92.

3.3 Fractography results

Fig. 10 shows the cross sectional area of SPC rupture specimen for the load of 450 N. The white marked circle area is a rupture part nearest to fracture surface and was observed by SEM.

The creep cavities were clearly observed at prior austenite grain boundaries in the cross section of creep ruptured part. This implies that the fracture of SPC was caused by creep cavity and shows the validity of SPC test.

4. Conclusions

To investigate the relation between uniaxial creep data and small-punch creep data, uniaxial and small-punch creep rupture tests on Grade 92 steel were performed at elevated temperatures and the behavior was studied. From the converted strain data derived on the modified Monkman-Grant relation, the relationship between the minimum creep rate from the uniaxial creep test and the minimum displacement rate from the small-punch creep test was found to be well established and, moreover, the validity of the alternative creep test method also could be confirmed. Also, it was verified that the fracture of SPC was caused by creep cavity.

ACKNOWLEDGMENT

This research was supported by Basic Science Research Program through the National Research Foundation of Korea(NRF) funded by the Ministry of Education, Science and Technology (No. 2011-0014946).

REFERENCE

1. Parker, J. D. and James, J. D., "Creep behavior of miniature disc specimens of low alloy steel," ASME PVP-Developments in a Progressing Technology, Vol. 279, pp. 167-172, 1994.
2. Ule, B., Šuštar, T., Dobeš, F., Milička, K., Bicego, V., Tettamanti, S., Maile, K., Schwarzkopf, C., Whelan, M. P., Kozłowski, R. H., and Klaput, J., "Small punch test method assessment for the determination of the residual creep life of service exposed components: outcomes from an interlaboratory exercise," Nuclear Engineering and Design, Vol. 192, No. 1, pp. 1-11, 1999.
3. Yoon, K. B., Park, T. G., Shim, S. H., and Jeong, I. S., "Assesment of creep properties of 9Cr steel using small punch creep test," Transactions of the KSME A, Vol. 25, No. 9, pp. 1493-1500, 2001.
4. Parker, J. D., Stratford, G. C., Shaw, N., Spink, G., and Metcalfe, H., "The Application of Miniature Disc Testing for the Assessment of Creep Damage in CrMoV Rotor Steels," BALTICA IV, Plant Maintenance, pp. 477-488, 1998.
5. Kim, B. J., Lim, B. S., and Ki, D. H., "Creep Behavior and Life Evaluation of Aged P92 Steel," International Journal of Modern Physics B, Vol. 20, No. 25n27, pp. 4231-4236, 2006.
6. Kameda, J., "Mechanical Properties of aluminized CoCrAlY coatings in advanced gas turbine blades," Materials Science and Engineering A, Vol. 234-236, pp. 489-492, 1997.
7. Tettamanti, S. and Crudeli, R., "Small Punch Creep Test: A Promising Methodology for High Temperature Plant Components Life Evaluation," In Baltica IV, Plant Maintenance for Managing Life & Performance, Vol. 2, pp. 501-509, 1998.
8. Wachter, O., Zabelt, K., Ennis, P. J., Helmrich, A., and Bohme, A., "The design, Manufacture and installation of a P92 header," Forschungszentrum Juelich Schriften Reihe Energietechnik, Vol. 5, No. 1, pp. 351-360, 1998.
9. Doveš, F. and Milička, K., "On the Monkman-Grant relation for small punch test data," Materials Science and Engineering A, Vol. 336, No. 1-2, pp. 245-248, 2002.
10. Yang, Z. and Wang, Z., "Relationship between strain and central deflection in small punch creep specimens," International Journal of Pressure Vessels and Piping, Vol. 80, No. 6, pp. 397-404, 2003.